

Star formation in Perseus

IV. Mass dependent evolution of dense cores.

J. Hatchell¹, G. A. Fuller²

¹ School of Physics, University of Exeter, Stocker Road, Exeter EX4 4QL, U.K.

² Jodrell Bank Centre for Astrophysics, Alan Turing Building, University of Manchester, Manchester M13 9PL, U.K.

Feb 08

ABSTRACT

Context. In our SCUBA survey of Perseus, we find that the fraction of protostellar cores increases towards higher masses and the most massive cores are all protostellar.

Aims. In this paper we consider the possible explanations of this apparent mass dependence in the evolutionary status of these cores. We investigate the implications for protostellar evolution and the mapping of the embedded core mass function (CMF) onto the stellar IMF.

Methods. We consider the following potential origins of the observed behaviour: dust temperature; selection effects in the submillimetre and in the mid-infrared observations used for pre/protostellar classification; confusion and multiplicity; transient cores; and varying evolutionary timescales. We develop Core Mass Evolution Diagrams (CMEDs) to investigate how the mass evolution of individual cores maps onto the observed CMF.

Results. We find that two physical mechanisms – short timescales for the evolution of massive cores, and continuing accumulation of mass onto protostellar cores – best explain the relative excess of protostars in high mass cores and the rarity of massive starless cores. In addition, we show that confusion both increases the likelihood that a protostar is identified within a core, and increases mass assigned to a core. Selection effects and/or transient cores also contribute to an excess of starless cores at low masses.

Conclusions. The observed pre/protostellar mass distributions are consistent with faster evolution and a shorter lifetime for higher-mass prestellar cores. We rule out longer timescales for higher-mass prestellar cores. The differences in the prestellar and protostellar mass distributions imply that the prestellar CMF (and possibly the combined pre+protostellar CMF) should be steeper than the IMF. A steeper prestellar CMF can be reconciled with the observed similarity of the CMF and the IMF in some regions if a second opposing effect is present, such as the fragmentation of massive cores into multiple systems.

Key words. Submillimeter; Stars: formation; ISM: clouds

1. Introduction

The stellar Initial Mass Function (IMF) *may* largely be determined in the prestellar phase of the evolution of dense cores, as the close agreement between the form of the prestellar core mass function (CMF) and the IMF enticingly suggests (Motte et al. 1998; Testi & Sargent 1998; Johnstone et al. 2000, 2001; Motte et al. 2001; Johnstone et al. 2006; Reid & Wilson 2006; Kirk et al. 2006; Nutter & Ward-Thompson 2007; André et al. 2007; Alves et al. 2007; Goodwin et al. 2007). However, feedback, competitive accretion and varying evolutionary timescales may all have a role to play in the evolution of the cores. Clearly, it is important to study how the mass in dense starless cores relates to the mass in cores forming protostars (protostellar cores), and therefore what determines the mass available to each protostar as it grows in mass.

There are now a number of molecular clouds for which the dense cores have been catalogued (from millimetre (mm) and submillimetre (submm) surveys) and classified (using the mid-infrared detections from the Spitzer Space Telescope). Perseus is one such cloud, for which we car-

ried out a submm survey with SCUBA (Hatchell et al. 2005, 2007b,a, hereafter Papers I–III, see also Kirk et al. 2006 and the similar 1300 μ m survey with Bolocam by Enoch et al. 2006). We have identified over 100 submm cores, each of which has been classified as starless or protostellar using Spitzer (Paper II, Jørgensen et al. 2006, 2007) and molecular outflows (Paper III).

An intriguing result in Perseus is that the highest mass cores are all protostellar (Fig. 1), and as one moves towards lower masses, an increasing fraction of cores appear to be starless. This leads to the obvious questions: why are there so few massive starless cores and why are the two distributions different? In this paper we address these questions. We start by first reviewing the results of the previous work on this cloud (Sect. 2), and consider the effects of the analysis of the submm data, detection limits and multiplicity on the distributions. Then in Sect. 4 we discuss some evolutionary scenarios which might produce these effects and introduce core mass evolution diagrams to illustrate how core evolution maps onto the observed CMF. In Section 5 we explore the factors which affect the relationship between the CMF and the IMF before presenting the summary and conclusions in Section 6.

2. Results

The 103 submm cores discussed here were identified using Clumpfind (Williams et al. 1994) on the SCUBA 850 μ m map of Perseus spatially prefiltered by removal of a 2' Gaussian smoothed background (primarily to remove artefacts from the image reconstruction; see Paper II for details). The identified cores have masses in the range 0.5–50 M_{\odot} , sizes ~ 0.1 pc (1' at the assumed 320 pc distance of Perseus), and mean H₂ densities of $> 3 \times 10^5$ cm⁻³.

In Paper II, we classified the cores using mid-IR detections from Spitzer to identify protostars. There are slight discrepancies between our classification and the embedded YSO list of Jørgensen et al. (2007), due to the different classification methods used (in our case, IRAC sources within 12'' or the Clumpfind source radius of the submm peak (see Paper II), whereas Jørgensen et al. (2007) looked for MIPS 24 μ m sources within 15'' of the peak). In total, 13 of our sources are classified differently by Jørgensen et al. (2007), but only one of our massive protostellar sources ($M > 1 M_{\odot}$) is reclassified as starless. The majority of the massive protostellar sources are well-known (L1448C, L1448 NW, NGC1333 IRAS 4A, HH211). Therefore the alternative classification does not significantly change the distributions. We found that the ratio of protostellar cores to starless cores increased with mass, with ultimately no starless cores at all at the highest masses (above 12 M_{\odot} , Paper I, Fig. 3). This result is shown in a modified form in the top panel of Figure 1 (Section 3.2).

In Paper III we used an alternative classification of the nature of the cores based on the presence or absence of molecular outflows for a subsample of 51 sources, and found the same result.

In fact these effects (the most massive cores are protostellar, with more starless cores at lower masses) have now been independently confirmed in Perseus by Enoch et al. (2008) using masses based on Bolocam 1.3 μ m data (Enoch et al. 2006), and the alternative Spitzer identification (Jørgensen et al. 2006; Rebull et al. 2007; Jørgensen et al. 2007; Lai et al. 2008). Enoch et al. (2008) also finds the same holds for Serpens, though intriguingly not Ophiuchus, which shows more similar mass distributions for starless and protostellar cores. The massive star-forming region Cygnus X shows a more extreme version of this effect, with no massive starless cores (Motte et al. 2007).

3. Assumptions and selection effects

Below we consider possible selection effects and assumptions which could influence our results and the core mass distributions.

3.1. Detection and Identification

The submm continuum detections are flux-limited. The observations are not sensitive to cores below a column density threshold of 8×10^{22} cm⁻² ($A_v \simeq 90$) (the 5 σ flux detection limit at 850 μ m). For a point source, this corresponds to a mass limit of 0.5 M_{\odot} (assuming 10 K and opacity $\kappa_{850} = 0.012$ cm² g⁻¹, see Paper II), but more massive sources can go undetected if the flux is more extended. Below this, our core detection is incomplete, and deeper studies are needed to determine the form of the mass distribution

(eg. the Orion metastudy by Nutter & Ward-Thompson 2007). The sensitivity and high anticipated source counts of the next generation of submillimetre surveys, such as the JCMT Gould's Belt Legacy Survey (Ward-Thompson et al. 2007) and Herschel survey of nearby star-forming regions (André & Saraceno 2005) will lay to rest incompleteness issues at the 0.1 M_{\odot} level in nearby clouds. But currently, with a relatively shallow column density detection limit, for many cores we must be only detecting the 'tip of the iceberg' with much of the mass lying at lower, undetectable column densities. In addition, objects over 2' (0.2 pc) in size are significantly affected by the spatial filtering of the data needed to removed artefacts on large size scales. The impact of the filtering depends on the degree of central concentration of a source with the less condensed sources being the most strongly suppressed.

For both these reasons (high column density detection threshold and filtering of extended cores) we are better at detecting cores with a high degree of central concentration, so the observations may only be tracing the later stages of prestellar evolution (eg. Tassis & Mouschovias 2004). For cores smaller than $\sim 2'$ in size, higher mass cores are easier to detect. A priori we might expect a selection effect which favours the detection of starless (and protostellar) cores with higher masses. So the lack of high-mass starless cores is not a consequence of our inability to detect them if they exist. The submm detection limits do not explain the lack of high-mass starless cores.

3.2. Temperature

In Paper II, the masses of the cores were calculated from the 850 μ m emission assuming a constant dust temperature of 10 K, which was the highest estimate for T_d consistent with all the spectral energy distributions (SEDs). However, protostellar sources tend to have higher temperatures and so produce relatively more 850 μ m emission for the same mass of circumstellar material. Can the assumed dust temperature reconcile the masses of the starless and protostellar cores?

In order to test this, we recalculate the masses for the sources assuming different dust temperatures. Recent studies of NH₃ found a small difference between *gas* temperatures of 11 and 12 K for starless and protostellar cores, respectively (Rosolowsky et al. 2007). However, differences in the dust temperature between starless and protostellar cores are evident from continuum observations of the SEDs of sources (Hatchell et al. 2007b; Enoch et al. 2008). The apparent difference between the gas and dust temperatures, averaged along the line of sight, is presumably due to the different sensitivity of molecular line and dust emission to the warmer inner regions of the sources. Modelling of prestellar and protostellar cores has found equivalent isothermal dust temperatures of $T_{\text{dust}} = 11$ K (starless), 14 K (Class 0 protostars) and 16 K (Class I protostars) (Evans et al. 2001; Shirley et al. 2002; Young et al. 2003).

We follow Enoch et al. (2006) in assuming 10 K for starless cores and 15 K for protostars, in order to ensure that we account fully for dust temperature differences. The mass distribution for our sources assuming 10 K and 15 K temperatures for the starless and protostellar sources respectively is shown in the upper panel of Figure 1. Although reduced from Paper II, due to the lower masses inferred for the protostellar sources, there is still a significant differ-

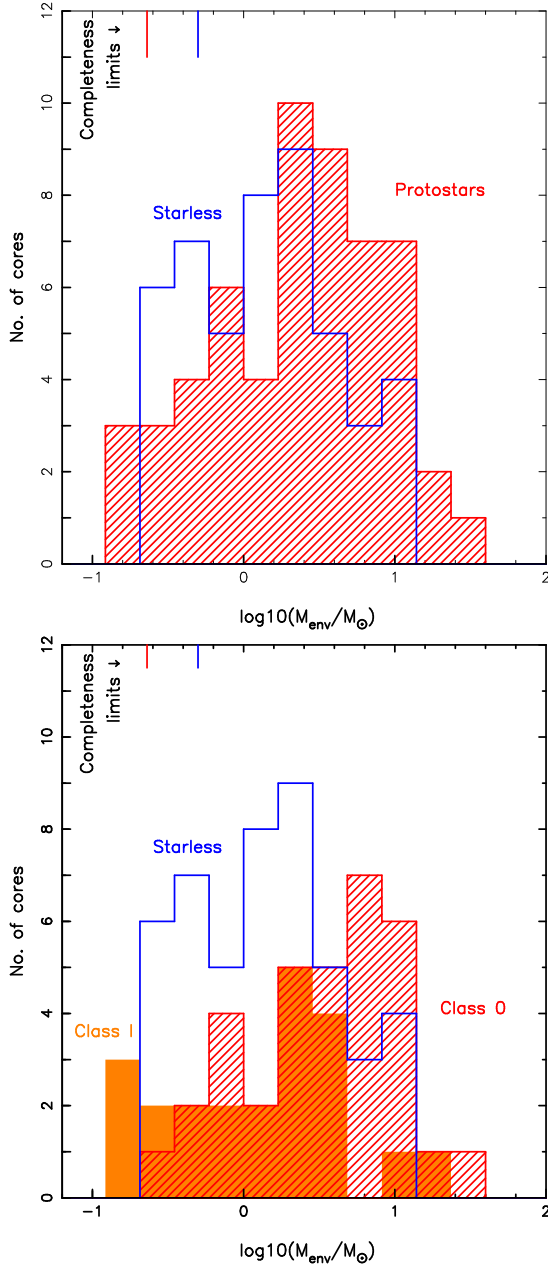


Fig. 1. Top: Histogram of masses of submm cores, assuming 10 K for starless cores (blue line) and 15 K for protostars (red hatched). The SCUBA completeness limits for point sources at each temperature are marked at the top of the plot. **Bottom:** As above with protostars separated into Class 0 (red hatched) and Class I (orange filled).

ence in the mass distribution of the starless and protostellar cores, with more protostellar sources at higher masses and more starless cores at lower masses. To quantify this, in the whole population 46% of sources are starless, but above $3 M_{\odot}$ this falls to 31%, 20% above $10 M_{\odot}$, and zero above $15 M_{\odot}$. A K-S indicates that the probability that these two samples are drawn from the same mass distribution is 4%, compared to 0.001% when a temperature of 10K is assumed for all the sources as in Paper II. Only considering sources above $1 M_{\odot}$, the K-S test gives a probability of 8% that the distributions are the same.

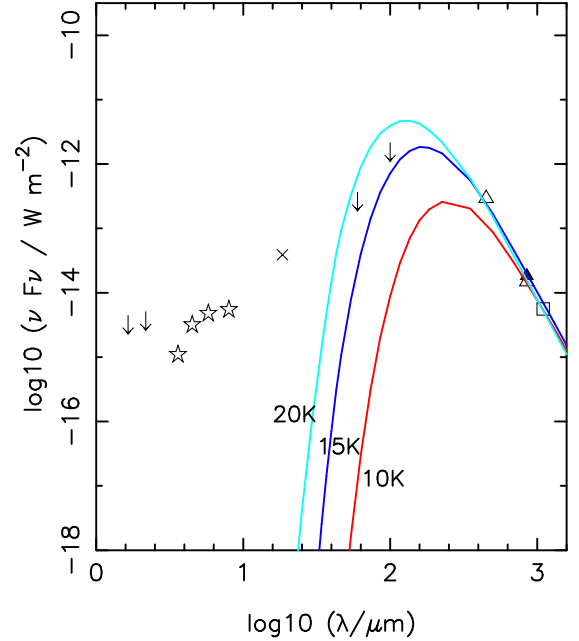


Fig. 2. Average SED for all 34 Class 0 sources overplotted with modified blackbodies at 10, 15 and 20 K. Flux points are the mean of all detections from Class 0 sources at each wavelength, from (left to right) 2MASS, Spitzer IRAC, Michelle, IRAS, SCUBA and Bolocam (see Paper II, for details). The 70 and 100 micron points are strictly upper limits because of potential confusion within the IRAS beam, but still constrain the maximum temperature to less than 20 K. The 2MASS datapoints are marked as upper limits as the high fluxes are likely due to confusing sources.

The lower panel of Figure 1 shows the core mass distribution but with the protostars separated into Class 0 and Class I evolutionary stages based on the classification in Paper II. As expected, the more evolved Class I cores have lower masses than the Class 0 sources. From this figure we see that the excess of protostars is mainly due to the excess of Class 0 cores, and therefore it is the temperature of the Class 0 population that is critical to the difference between the prestellar and protostellar mass distributions. Since the sense in which the mass distributions differ is that the Class 0 sources are more massive, this difference could be reduced if the Class 0 sources had even higher temperatures. Raising the assumed temperature to 20 K for the Class 0 sources would produce a distribution more compatible with that of starless cores (15% K-S probability). However, a temperature as high as 20 K (which would be larger than the temperature of the Class I sources) is ruled out by the individual SEDs, including those of the most massive Class 0 cores (Paper II). The average SED for the Class 0 cores is shown in Fig. 2. As the model SEDs show, the observations are compatible with a temperature of 15 K but not 20 K. Therefore even taking temperature into account, there is still a significant difference between the two mass distributions.

A consequence of assuming a temperature of 15 K rather than 10 K is that a given $850\mu\text{m}$ flux corresponds to a factor 2 lower column density. As Clumpfind integrates mass down to a fixed flux limit, the mass of higher temperature gas is measured down to a lower column density than lower temperature gas. If temperatures at the outer edges

of protostars are significantly higher than those for starless cores, this creates a bias towards higher masses for protostars as surrounding material at lower column densities is included than for starless cores. To quantify this effect requires an understanding of the temperature structure of the cores. The 15 K and 10 K values are the mass-weighted average in the beam, with the higher value for protostars due to the central heating. At large radii, the temperatures of protostars and starless cores are more similar. Models suggest that temperatures fall to below about 12 K within 10,000 AU ($30''$) of the central protostar and both starless and protostellar cores are heated to 12–14 K at their outer edges by the interstellar radiation field (Evans et al. 2001; Shirley et al. 2002), suggesting that this possible bias is not likely to produce a significant systematic effect.

In addition to the different mass distributions of the protostellar and starless cores, a slightly different question is whether there is a significant excess of protostars associated with higher mass cores. Above $10 M_{\odot}$, only 2 out of 10 sources are starless. Applying the binomial distribution, the probability of getting 2 or fewer starless cores by chance is 9.3%. Although not entirely impossible that this is a random fluctuation (and we are limited here by the small number of high mass objects in one cloud), the overpopulation of protostars at high masses is likely to be real. This is further supported by the excess of high mass protostars also found in Serpens (Enoch et al. 2008).

3.3. Source Confusion

The absence of massive starless cores could result from source confusion, if our analysis erroneously fails to separate multiple lower mass cores, one of which happens to contain a protostar. This could occur due to insufficient angular resolution, or overlapping cores along the line of sight. Both of these are potentially more significant issues in regions where cores and protostars are clustered, such as NGC1333 and IC348.

The 10 most massive protostellar cores in our sample are all in clusters or groups (B1, IC348, L1448, NGC1333). This is consistent with the expectation that massive stars form in clusters. We might also expect to find the most massive prestellar cores in clusters. Yet only two of the four most massive prestellar cores are in NGC1333; the other two are the filaments to the SW of B1 and the SE of L1448, outside the main clusters of protostars. It is possible that we fail to identify starless cores in clusters because they are confused with existing protostars. Many of the most massive cores contain multiple protostars: L1448 NW, NGC1333 IRAS 4A and 4B, NGC1333 IRAS 2A/B. The core B1-b contains multiple submm peaks (Hirano et al. 1999) but only one object is identified as a protostar.

In clusters, it is often unclear how to share the mass in the dense, fragmenting filaments between individual objects. Multiplicity clearly affects our ability to identify, at the prestellar and protostellar stage, the amount of mass which ultimately will contribute to one star. As protostars produce strong peaks, and all clumpfinding software looks for peaks, some prestellar material may be being attributed to nearby protostars, increasing the mass of the protostellar cores at the expense of starless cores. Thus, confusion could explain why we identify the most massive protostellar cores in clusters. However, it does not explain why only the more massive starless cores are underabundant with respect to

protostars, as we would expect at least as many lower-mass starless cores to be lost due to confusion.

3.4. Stellar Content

The difference between the mass distributions also depends on our ability to differentiate protostars from starless cores. For protostars, luminosity and outflow power decrease with decreasing mass (Bontemps et al. 1996; Fuller & Ladd 2002), and therefore both the MIR and CO outflow emission become weaker. The mid-IR and outflow detection limits could therefore explain why there are more apparently starless cores at lower masses.

The Spitzer c2d survey (Evans et al. 2003) is limited in the lowest luminosity source it can detect. The Spitzer detections for the lowest-mass sources identified as protostars are all close to the IRAC detection limits and the addition of MIPS-only detections increases the number only by a few (Rebull et al. 2007; Jørgensen et al. 2007). Spitzer c2d is estimated to be 100% complete to a luminosity of $0.3 L_{\odot}$ in Serpens (Harvey et al. 2007) though significant fractions of lower-luminosity sources are detected (e.g. Dunham 2007), with 50% completeness at $0.01 L_{\odot}$. We can assume these limits also apply to Perseus, as it is at a similar distance. So the population of protostars in Perseus with $L < 0.3 L_{\odot}$ remains incompletely sampled by Spitzer. For reference, a luminosity limit of $0.3 L_{\odot}$ implies completeness to sources above $1 M_{\odot}$ final stellar mass, according to the PMS tracks of Siess et al. (1999) (assuming constant accretion). Some of the low-mass starless cores could contain undetected low-luminosity MIR sources and this will only be resolved by further deep searches in the MIR, such as with *Herschel* (André & Saraceno 2005).

In Paper III we considered in detail the detection statistics for outflows and concluded that the outflow observations also do not conclusively rule out the presence of low mass, low luminosity protostars in the apparently starless cores. Subsequent observations suggest that the majority of the cores are indeed starless, i.e. they do not contain outflows, when a deeper (by factor > 5) outflow search is carried out (Hatchell et al. in prep.).

Nonetheless, although incompleteness might explain an excess of starless cores, it can only increase the fraction of starless cores as compared to protostars. In particular the failure of MIR and outflow observations to detect low-luminosity sources cannot explain why all the most massive cores are protostellar.

3.5. Transient cores

A population of transient cores, cores which are not gravitationally bound, might contribute to explaining the overpopulation of low-mass starless cores. A population of failed cores which will not form protostars or transient starless cores which increases at lower masses was suggested by Elmegreen (1997) and is seen in turbulence simulations (Padoan & Nordlund 2002; Vázquez-Semadeni et al. 2005). Cores whose chemistry suggests transience are also observed (Morata et al. 2005).

Estimates of the fraction of cloud mass in dense cores range from a few percent (Fuller & Myers 1987; Johnstone et al. 2004; Motte et al. 1998) to a few tens of percent (Paper I), typically with uncertainties of more

than a factor of two. Ultimately, the mass expected to end up in stars is also few percent of the total cloud mass (Lada & Lada 2003), suggesting that in some cases there will be little mass in the core budget which does not ultimately go in to stars.

It has been argued that cores that are centrally condensed enough to be detected in the submm must be forming stars and therefore are not transient (Motte & André 2001). With high mean densities above $n_{H_2} \sim 3 \times 10^5 \text{ cm}^{-3}$, corresponding to a thermal Jeans mass of $0.3 M_\odot$, our sources contain from one to tens of Jeans masses and thus satisfy the minimum condition to be gravitationally bound. On the scales probed by the N_2H^+ line (critical density 10^5 cm^{-3}), linewidths are roughly thermal and the majority of cores are virially supported if an external pressure term is included (Kirk et al. 2007a). It therefore seems unlikely that we are seeing a large population of unbound objects. However, it is possible that some cores could be destroyed by future energetic events, particularly cores in disruptive cluster regions, or that the currently binding external pressure decreases to the point where cores re-expand, particularly for lower-mass cores.

4. Core mass evolution

The observed prestellar and protostellar core mass functions are built up of mass measurements of many individual sources. To fully understand them we must consider how individual objects evolve and how they appear to the observer at different times. By modelling the mass evolution of cores, and reflecting this in the CMF, we have a tool to investigate how different factors in core evolution can lead to differences in the observed CMFs.

One possibility is that the timescale for forming a star, t_{sf} , may be dependent on core mass. As the number of prestellar or protostellar objects is the product of the production rate and the lifetime, longer lifetimes in a particular phase imply a greater number of detections and a large representation on the CMF.

A second factor is the relationship between the time it takes a core to form a star, and the time it takes for the core to grow in mass. The important parameter here is the ratio the timescale for a core of a given mass to form a protostar (t_{sf}) to the timescale for the core mass to grow through the accretion of additional material from its surrounding cloud, (t_{gr}). In the limit $t_{\text{sf}} \ll t_{\text{gr}}$, a core can be considered as being fixed mass reservoir while it is forming stars.

On the other hand, if $t_{\text{sf}} \gtrsim t_{\text{gr}}$, star formation will be taking place within a core as the core continues to grow in mass. These two scenarios have different implications for the relationship between the mass distributions of starless and protostellar cores.

4.1. Core mass evolution and the CMF

The detectable mass of starless cores and protostars changes as they evolve, so that each object moves across a range in observable masses during its lifetime, and the CMF is an average of sources at different stages in their evolution. Prestellar cores start as diffuse objects below the column density detection limits of submm surveys such as this one (see Sect. 3.1), and become more centrally condensed with time so that the detectable mass starts at the detection

threshold and rises throughout the prestellar phase. For example, in the seminal collapse calculation of Larson (1969), detectable central densities of $3 \times 10^5 \text{ cm}^{-3}$ are reached after $2 \times 10^5 \text{ yr}$ and the mass above the detection threshold continues to rise until a central core is formed at $5 \times 10^5 \text{ yr}$. For protostellar cores, outflows and accretion remove mass, and the Class I sources have lower masses than Class 0s (Fig. 1).

To represent this graphically we can plot Core Mass Evolution Diagrams (CMEDs, Figs. 3 and 4) which show mass vs. time for various models of core evolution, and the resulting core mass functions. For example, in Fig. 3a we plot the evolution of a core with a simple linear evolution of mass with time, given by

$$m(t) = m_{\text{peak}}(1 - |t|/T), \quad (1)$$

where m_{peak} is the maximum mass reached by the core, $t = 0$ is the time at which a protostar forms, and $T = 0.5 \text{ Myr}$ the timescale for core growth or mass loss. This represents the accumulation of mass above the detection threshold during the prestellar phase, and loss of mass through accretion and outflow as a protostar. For this model, the time for core growth and the time for a star to form are equal: $t_{\text{sf}} = t_{\text{gr}}$. If we take a population of such cores and observe them at random times then we generate the CMD shown in the lower panel. The CMD is a power law with a positive index of +1, reflecting the longer times spent in the higher mass bins (which are equal width in $\log_{10}(m)$).

Likewise, Fig. 3b shows cores with evolution given by

$$m(t) = m_{\text{peak}}(|t|/T + 1)^{-1/\gamma} \quad (2)$$

with $\gamma = 1.35$ and $T = 10^4 \text{ yr}$. The resulting CMF is a power-law with negative index -1.35 . This function, with longer timescales at lower masses, is the pathological case where time evolution alone reproduces a Salpeter-like CMF from a single population of identical sources. This mass evolution function becomes unrealistic at low masses because the timescales tend towards infinite (note the apparent sharp cutoff at $\log_{10}(M/M_\odot) = -0.85$ is simply the mass reached at the time limits of our calculation). Nonetheless this, or a similar form for the mass evolution of cores, is interesting as it produces a CMF with a power-law slope at the high mass end similar to the slope of the IMF. Also, it implies a protostellar mass loss rate which peaks early in the protostellar stage and then decreases with time in line with decreasing outflow mass loss (Bontemps et al. (1996), but see also Paper III).

In such a model, all stars would form inside high mass cores, with low mass stars produced in multiples or with low efficiency. The strongest evidence against such a scenario is the existence of low-mass low-luminosity Class 0 sources, some of which have small outflows supporting their youth (Hatchell et al. 2007a; Dunham 2007). A single peak core mass model is clearly extreme. However, a population of low-mass cores on the CMD in itself does not imply that protostars form in low mass cores.

To generate more realistic diagrams we assume a population of cores with a distribution of peak (maximum) masses m_{peak} following a three-part power-law (the peak core mass function or PCMF):

$$dN(m_{\text{peak}})/d\log(m_{\text{peak}}) \propto m_{\text{peak}}^{-(\alpha-1)} \quad (3)$$

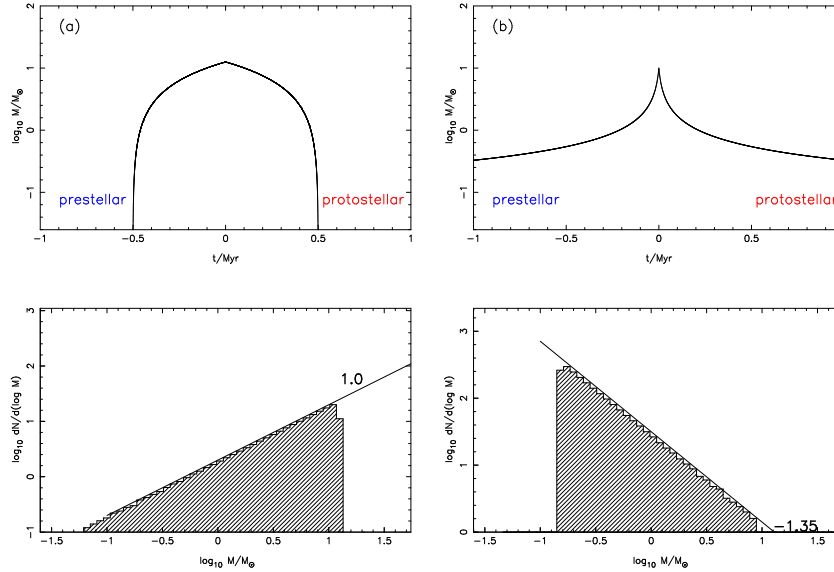


Fig. 3. Core mass evolution diagrams (CMEDs) for single evolutionary tracks. Each top panel shows on a linear-log plot the evolution of the core mass (as measured above a detection threshold) as a function of time. The bottom panels show the corresponding core mass functions assuming a population of identical cores sampled at random times. **(a):** Linear core mass evolution. **(b):** The pathological case where a population of identical cores results in a Salpeter power law CMF simply through mass evolution governed by Equation 2.

with

$$\begin{aligned} \alpha = 0.3 & \quad 0.2 < m_{\text{peak}} \leq 0.8 & \quad (-0.7 < \log_{10} m_{\text{peak}} \leq -0.1) \\ \alpha = 1.3 & \quad 0.8 < m_{\text{peak}} \leq 5.0 & \quad (-0.1 < \log_{10} m_{\text{peak}} \leq 0.7) \\ \alpha = 2.3 & \quad 5.0 < m_{\text{peak}} & \quad (0.7 < \log_{10} m_{\text{peak}}). \end{aligned}$$

The boundaries between the power law segments are set a factor of 10 higher in mass than those for the Galactic field IMF (Kroupa 2002) to take into account the star formation efficiency (Nutter & Ward-Thompson 2007; Alves et al. 2007). The peak core mass function is significant because it gives the total mass available to each protostar for accretion, which relates directly to the IMF through the SFE (see Sect. 5).

We then generate CMFs based on this distribution under various assumptions about the evolution of the core mass with time. From the core mass evolution we calculate the core mass function assuming that the ensemble of cores is observed at random points during their evolution. The observed population on the CMF in a given mass range is a sum over the population of cores of the time spent in that mass range.

In the simplest case (Fig. 4a), we assume that the measured mass above the detection threshold increases at a constant rate in the prestellar phase, and decreases at a constant rate in the protostellar phase, following Equation 1. The timescales for core growth and protostellar formation are equal, $t_{\text{gr}} = t_{\text{sf}} = T$. For this simple case the observed CMF is similar to the underlying peak mass function in that it shows a 3-part power law above $0.2 M_{\odot}$. However, the power-law indices of 0.25, -0.4 and -1.35 are steeper than those of the underlying peak core mass function ($0.7, -0.3, -1.3$ in $\log m_{\text{peak}}$) because of the contribution of evolving cores detected at less than their maximum mass. This contribution increases towards lower masses, particularly where the underlying mass function has turned over, and

also explains the population below $\log_{10} m = -0.7$ with index $+1$ which does not exist in the PCMF.

Using CMEDs we can now investigate the effects of different evolutionary scenarios on the observed CMF.

4.2. Fast evolution of massive cores

The lack of massive starless cores, and the decrease in the number of starless cores towards higher masses, could imply that more massive cores have relatively short prestellar lifetimes, and that this is why we see few of them. (The alternative, that higher-mass protostars have longer lifetimes, can not explain why so few massive starless cores are detected). Current best estimates for the mean lifetime for starless cores detectable in the submm are similar to the protostellar lifetime, $1.5\text{--}4 \times 10^5$ years (Hatchell et al. 2005; Enoch et al. 2007; Kirk et al. 2007b), but the free-fall timescales for mean densities of $> 3 \times 10^5 \text{ cm}^{-3}$ are less than 7×10^4 years, so theoretically this observed phase could be very short.

From the observations we can estimate the prestellar to protostellar ratio for cores at masses above $10 M_{\odot}$: there are four times as many protostars suggesting a prestellar lifetime $1/4$ of that in the protostellar phase. For comparison, at $3 M_{\odot}$ the number of cores in the prestellar and protostellar phases are roughly equal.

In Fig. 4b we plot a CMED in which massive cores evolve fast in the prestellar phase, with mass evolving linearly with time according to Equation 1 but with varying prestellar timescale $T = 1/\sqrt{m_{\text{peak}}/M_{\odot}}$ Myr. The protostellar timescale remains constant at $T = 0.5$ Myr. The resulting prestellar mass distribution is steeper than the core peak mass function (steeper than $m^{-1.35}$) and steeper than the (unchanged) protostellar mass distribution. Therefore we can reproduce the excess of high-mass protostars by assuming protostellar lifetimes are all equal but the prestellar lifetimes depend strongly on mass, with short lifetimes for

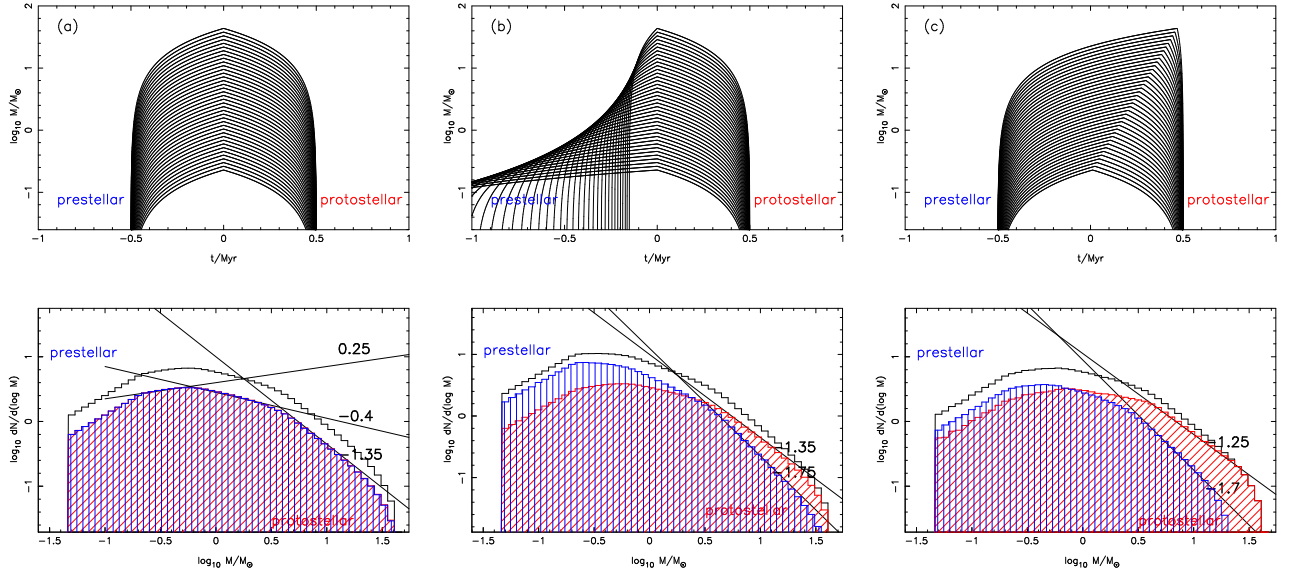


Fig. 4. Core mass evolution diagrams (CMEDs) for different evolutionary scenarios. Each top panel shows the evolution of core masses as measured above a detection threshold as a function of time for various peak masses m_{peak} , on a linear-log plot. The bottom panels show the corresponding time-averaged core mass functions for prestellar cores (blue, vertical hatching), protostellar cores (red, diagonal hatching), and all cores (thin solid line). The straight lines are marked with approximate power laws for sections of the CMF. **(a)** Equal pre/protostellar timescales for all cores regardless of mass, with a constant mass accumulation/removal rate $\pm \dot{m} \propto m_{\text{peak}}$. **(b)** Faster evolution for more massive sources in the prestellar phase only. **(c)** Continuing accretion into the protostellar phase, so that the peak mass is reached some time after $t = 0$.

high mass sources. Note that this model still forms stars at the point at which the core stops growing, $t_{\text{sf}} = t_{\text{gr}}$.

Longer prestellar lifetimes for lower-mass cores are predicted by ambipolar diffusion models (Tassis & Mouschovias 2004), and our results are qualitatively consistent with this. Starting from the assumption that higher mass cores evolve from lower density (hence have a higher Jeans mass), Clark et al. (2007) find the opposite: that the free-fall timescale is longer for higher mass cores, and therefore the prestellar mass distribution should be flatter than the IMF. Our result differs from that presented by Clark et al. (2007) because our cores evolve in mass during the prestellar and protostellar phase, so there are differences in how the observed CMF is derived. Nonetheless, longer timescales for higher mass clumps are inconsistent with our results.

The above discussion assumes that cores evolve at fixed (gas+stellar) mass, ie. the timescales for star formation are much less than the timescales for acquisition of additional material by the cores, $t_{\text{sf}} \ll t_{\text{gr}}$. In this case the difference in mass distributions argues that massive cores must themselves form and then evolve to form stars more rapidly than low mass cores.

4.3. Continuing accretion

In a model where the core is not considered to be a fixed mass reservoir but continuing accumulation of mass is allowed during the protostellar phase, the envelope mass can continue to rise during the main protostellar accretion phase. This is the case where the star formation timescale is less than the timescale for core growth, $t_{\text{sf}} < t_{\text{gr}}$. The peak envelope mass can then be reached sometime during the protostellar phase rather than at the prestellar/protostellar

transition. Such models require surrounding lower-density material to become gravitationally bound to the core and continue to flow onto the envelopes of existing protostars.

A model of this is shown in the CMED in Fig. 4c. In this case, the time at which the peak core mass is reached is shifted into the protostellar phase by an amount proportional to $\log_{10} m_{\text{peak}} - \log_{10} m_{\text{min}}$ where $m_{\text{min}} = 0.2M_{\odot}$ is the minimum mass in the peak core mass function, so $t_{\text{gr}} \geq t_{\text{sf}}$. The resulting prestellar mass distribution is steeper than the peak mass function and steeper than the combined (pre+protostellar) CMF. The protostellar mass function is flatter, reflecting the reduced amount of time spent at low masses. Again, this model reproduces the main features of the observed pre/protostellar mass distributions. Core masses which continue to rise into the protostellar phase can explain why protostellar cores tend to have masses higher than those of starless cores.

Core masses will continue to increase into the protostellar phase as long as the mass loss through accretion and outflows is outweighed by mass moving from low density at large radii to within the column density detection threshold of the observations. Although the model in our CMED is clearly simplistic, there are several ways in which this kind of behaviour can arise. Recent models of core growth through ambipolar diffusion show significant inward velocities in the outer parts of the core which continue after the central protostar has formed (Adams & Shu 2007). Alternatively, if large-scale turbulent flows supply the cores (see Mac Low & Klessen 2004) then cores will continue to grow until the supply of material is exhausted. Additionally, in competitive accretion models, cores which have already accumulated higher masses form deeper gravitational wells and competitively accrete gas from the surrounding cloud and lower mass cores, which might bias the

growth towards already massive protostars (Bonnell et al. 2001, but note that there are kinematic arguments against competitive accretion: Walsh et al. 2004; André et al. 2007; Jørgensen et al. 2007; Kirk et al. 2007a, though see also Ayliffe et al. 2007).

4.4. Luminosity constraints on mass evolution

The bolometric luminosity is plotted against core mass for the Perseus sources in Paper II, Fig. 4 (protostars) and Paper III, Fig. 2 (all sources). There is a general trend of increasing luminosity with increasing mass, but with a large scatter. There are sources with an order of magnitude difference in core mass (the complete sample spans $0.5\text{--}50 M_{\odot}$) that produce similar bolometric luminosities while there is an order of magnitude scatter in source luminosity over some ranges of core mass. In principle the observed luminosity-core mass distribution provides a constraint on the evolution of the core mass and hence the CMF, but exploring this is complex.

The mass evolution of cores affects the luminosity of the protostars forming in the cores through accretion of core material onto the central star-disk system. The accretion luminosity is given by $L_{\text{acc}} = GM_*\dot{M}_{\text{acc}}/R_{\text{acc}}$ where M_* is the stellar mass, and \dot{M}_{acc} and R_{acc} are the accretion rate onto the star/disk and the accretion radius respectively. However to predict the luminosity evolution of the sources requires an understanding of how the accretion rate onto the star/disk \dot{M}_{acc} and the rate of change of mass of the core \dot{m} are related. This relationship is likely to be both complex and evolving. In addition to the mass loss due to accretion on to the central source, \dot{m} encompasses all the other core mass loss, and growth, mechanisms. This includes, for example, the mass loss associated with the effect of winds and outflows (not necessarily self-generated) as well as the growth of the core due to the accretion of surrounding cloud material. So for example, in the case where a core continues to grow in mass once a protostar has formed, \dot{M}_{acc} and \dot{m} have opposite signs up until the point when the core ceases to grow in mass. Even in the simple case where \dot{M}_{acc} is a constant fraction of \dot{m} , the radius into which the material falls, R_{acc} , and hence L_{acc} , is likely to evolve, as, for example, a circumstellar disk forms and grows, and core material of different angular momentum is accreted.

Using various simplifying assumptions and initial conditions, this luminosity evolution has been modelled by a number of authors (Smith 2000; Froebrich et al. 2006; Myers 1998; Siess et al. 1997; Saraceno et al. 1996). However these models have mostly concentrated on cores which contain a fixed reservoir of material and have not investigated the evolution of cores as massive the most massive cores observed in Perseus. It would be interesting to extend such models to encompass both the range of core masses seen in Perseus and possible alternative scenarios for the evolution of the core mass, but such models are beyond the scope of this paper.

5. From CMF to IMF

So far we have discussed how the observed core mass distributions relate to the underlying peak core mass distribution, and how differences between the mass distributions of

the prestellar and protostellar cores might arise. The subsequent issue is how these cores go on to form stars with a range of masses consistent with the IMF.

Observational selection effects and systematic errors (Section 3), as well as small number statistics (Swift & Williams 2008), make current measurements of the CMF highly uncertain. Nonetheless, the apparent similarity of the power-law slope of the CMF and the IMF has now been noted in several regions. The simplest explanation for the match is that *i*) there is a one-to-one mapping between cores and stars which are formed, *ii*) there is a uniform star formation efficiency (SFE) for all the cores i.e. that the same fraction of the mass of each core is converted in to star, *iii*) the measured mass of each core is representative of the total mass available to form a star, and *iv*) the evolutionary timescales are independent of the core mass.

If any of these assumptions is not in fact true, then the mapping of the CMF to the IMF of the stars formed is clearly more complex. However we can consider breaking each assumption in turn and examine how the resulting IMF relates to the CMF as measured for prestellar cores and/or all submm cores.

5.1. One-to-one mapping

Multiplicity breaks the one-to-one mapping between cores and stars. This has been considered in detail recently by Goodwin et al. (2007) and Swift & Williams (2008), who demonstrate that if multiplicity is significant we would expect the CMF to be skewed to higher masses compared to the IMF, as massive cores contribute to a final population of lower-mass stars. Goodwin et al. (2007) argue that the best match between the observed CMF (Nutter & Ward-Thompson 2007) and the IMF (Kroupa 2002) occurs if all cores (including low-mass cores) form binaries or higher-order multiples.

There is plenty of evidence for multiplicity in Perseus sources. Although multiple Spitzer MIPS sources can only be identified in 3 cores (Jørgensen et al. 2006), at least 10% of the SCUBA cores have been demonstrated to contain multiple sources when observed with high-resolution infrared, radio or mm/submm interferometry (Lay et al. 1995; Anglada et al. 2000; Rodríguez et al. 1997; Rodríguez & Reipurth 1998; Wolf-Chase et al. 2000; O’Linger et al. 2006; Hirano et al. 1999), and the majority of the submm sources have not been the targets of detailed studies of their fragmentation and multiplicity.

A population of cores which will never form stars, transient cores, would also break the one-to-one mapping between observed cores and stars. Transient cores are more likely to appear at low mass, where the gravitational binding is weaker, and skew the CMF to lower masses than the IMF. The presence of a population of low-mass, transient cores cannot be ruled out by our data.

5.2. Star formation efficiency

If the star formation efficiency (SFE) is not independent of core mass, variations in it can have a complex effect on the relationship between the CMF and IMF. Changes in the SFE can lead to an IMF which is either steeper or flatter than the CMF or affect different mass ranges differently,

depending on exactly how the SFE varies with core mass (Swift & Williams 2008), if indeed the SFE is an unique function of core mass at all. SFE variation therefore acts to skew or blur the relationship between the CMF and the IMF.

Although there are estimates of the instantaneous star formation efficiency in cores in Perseus of 10-15% (Jørgensen et al. 2007), we have no information on the variation in SFE between cores. Future constraints on the SFE may come from studying the mass transfer through accretion and outflows and probing how feedback processes affect star formation within a core.

5.3. Representative mass measurements

If the core masses measured are not representative of the total mass available for accretion over the lifetime of the core, then the relationship between the IMF and the CMF is again more complex. As discussed in Sec. 4.1, the observed mass of a core (or distribution of masses of a sample of cores) is a function of the peak mass of the cores and the time evolution of their mass. Depending on these two factors, different ranges of observed core masses may contribute to the same range of stellar masses in the IMF. In general cores will be observed at masses less than their peak mass, skewing the CMF to lower masses compared to the IMF. Only if cores spend a large fraction of their evolution with masses at, or near, their peak mass is the observed mass of core representative of the total mass available to form stars, leading to a one-to-one relationship between the IMF and CMF.

5.4. Evolutionary timescales

Longlasting evolutionary phases will be relatively overrepresented in the count of cores on the CMF. Conversely, the most rapid phases are the least likely to be seen. Therefore, if cores of different peak masses evolve at different rates, the shape of the CMF is affected. This is in contrast to the IMF, which takes account of the short lifetimes of massive stars by means of stellar evolution theory.

The evidence presented here for the absence of massive prestellar cores in the CMF can be explained if cores with high peak masses evolve more rapidly. Therefore, from the observed deficit of massive prestellar cores we would expect the IMF to be flatter (higher populations at higher masses) than the CMF.

Putting all four factors together, what can we say about the relationship between the measured CMF and the IMF? It is clear that if high-mass prestellar cores are underrepresented on the CMF, and cores map onto the IMF one-to-one with a constant core star formation efficiency, then we would expect the measured CMF to be steeper than the IMF at the high-mass end. At the low mass end, the CMF always contains an additional population of cores evolving to or from higher masses and should always be overpopulated relative to the IMF. To reconcile the observed similarity between the CMF and the IMF, it would be necessary to invoke two opposing effects, eg. faster evolution for more massive cores combined with multiplicity, which contrive to cancel out so that the observed CMF once again, and coincidentally, has the same power-law form as the IMF.

6. Summary and conclusions

The mass distributions of the prestellar and protostellar cores in Perseus are different, with an excess of protostellar cores at high masses and an excess of starless cores at low masses. There are a number of possible selection effects which could be influencing the observed distributions. Of these, only confusion in regions where cores and protostars are highly clustered can plausibly explain the observed distributions.

In clustered regions there is a difficulty in identifying the structures which will ultimately form a star. This may be because the gas which will go on to form future stars lies in dense, filamentary structure with no clear boundaries segregating it into discrete, centrally peaked cores. Confusion in the observations then leads to both an undercounting of starless cores and also an overattribution of mass to protostars if they are confused with essentially prestellar material.

Of the other assumptions and selection effects involved in deriving the mass distribution, differences in the temperatures between classes of cores cannot explain the differences between the mass distributions. At low masses, the distributions are affected by selection effects, particularly our increasing inability to identify low-luminosity sources as protostellar. Transient cores may also contribute to the excess of starless cores at low masses, but seem unlikely to be significantly influencing the relative underabundance of massive starless cores.

If selection effects are not the most significant cause of the difference in mass distributions, then these differences must be direct consequence of the evolution of cores. By looking at the mass distributions of the prestellar and protostellar cores separately, we can place constraints on core mass evolution. We find two evolutionary scenarios which explain the observed excess of protostellar cores with high masses. The simplest is that timescales for the formation of protostellar cores may vary with core mass, with more massive cores forming protostars more quickly than lower mass cores. Alternatively (or additionally), the masses above our column density threshold may continue to rise well into the protostellar phase, rather than peaking at the point when a protostar is formed. The observed distributions rule out the possibility that higher mass cores evolve more slowly to form protostars than lower mass cores.

Whatever the explanation for the observed differences in the mass distributions, they provide a clue to how cores evolve to form stars, and how the measured CMF relates to the stellar IMF. The relationship between the CMF and the IMF is in general complex and several assumptions about evolution, detectability and efficiencies have to be made to derive the IMF from the CMF. But clearly if we are undercounting the number of massive starless cores which form, either because they only last a short time or because of confusion with protostars, then the IMF should contain more systems at the high mass end of the distribution than the prestellar CMF. The IMF should also show relatively fewer sources at the low mass end compared to the CMF, because the CMF contains a contribution from cores observed while evolving to or from their maximum mass. On the other hand, we know that many cores will fragment into multiple lower-mass systems on the IMF (see Goodwin et al. 2007). In some clouds these effects may conspire to cancel each other, producing a CMF and an IMF with similar shapes.

Clouds such as Perseus where the distribution of prestellar and protostellar core masses are inconsistent with an apparently simple, direct mapping of the CMF to IMF provide important insights into the possible evolution of cores as they form stars. Deeper extensive surveys of cores and protostars in other clouds are needed to help unravel the details of these possible evolutionary paths of the cores.

Acknowledgements. The authors would like to thank Nicolas Peretto and Daniel Price for useful discussions, and referee Doug Johnstone for suggestions which significantly improved the paper. The James Clerk Maxwell Telescope is operated by the Joint Astronomy Centre on behalf of the Science and Technology Facilities Council of the United Kingdom, the Netherlands Organisation for Scientific Research, and the National Research Council of Canada. This work is based in part on observations made with the Spitzer Space Telescope, which is operated by the Jet Propulsion Laboratory, California Institute of Technology under a contract with NASA. JH acknowledges support from the PPARC (now STFC) Advanced Fellowship programme.

References

- Adams, F. C. & Shu, F. H. 2007, *ApJ*, 671, 497
- Alves, J., Lombardi, M., & Lada, C. J. 2007, *A&A*, 462, L17
- André, P., Belloche, A., Motte, F., & Peretto, N. 2007, *A&A*, 472, 519
- André, P. & Saraceno, P. 2005, in *ESA Special Publication*, Vol. 577, *ESA Special Publication*, ed. A. Wilson, 179–184
- Anglada, G., Rodríguez, L. F., & Torrelles, J. M. 2000, *ApJ*, 542, L123
- Ayliffe, B. A., Langdon, J. C., Cohl, H. S., & Bate, M. R. 2007, *MNRAS*, 374, 1198
- Bonnell, I. A., Bate, M. R., Clarke, C. J., & Pringle, J. E. 2001, *MNRAS*, 323, 785
- Bontemps, S., André, P., Terebey, S., & Cabrit, S. 1996, *A&A*, 311, 858
- Clark, P. C., Klessen, R. S., & Bonnell, I. A. 2007, *MNRAS*, 379, 57
- Dunham, M. M. 2007, in *American Astronomical Society Meeting Abstracts*, Vol. 211, 89.26
- Elmegreen, B. G. 1997, *ApJ*, 486, 944
- Enoch, M., Evans, N. I., & coauthors. 2008, in prep.
- Enoch, M. L., Glenn, J., Evans, II, N. J., et al. 2007, *ApJ*, 666, 982
- Enoch, M. L., Young, K. E., Glenn, J., et al. 2006, *ApJ*, 638, 293
- Evans, N. J., Allen, L. E., Blake, G. A., et al. 2003, *PASP*, 115, 965
- Evans, II, N. J., Rawlings, J. M. C., Shirley, Y. L., & Mundy, L. G. 2001, *ApJ*, 557, 193
- Frederich, D., Schmeja, S., Smith, M. D., & Klessen, R. S. 2006, *MNRAS*, 368, 435
- Fuller, G. A. & Ladd, E. F. 2002, *ApJ*, 573, 699
- Fuller, G. A. & Myers, P. C. 1987, in *NATO ASIC Proc. 210: Physical Processes in Interstellar Clouds*, 137–160
- Goodwin, S. P., Nutter, D., Kroupa, P., Ward-Thompson, D., & Whitworth, A. P. 2007, *ArXiv e-prints*, 0711.1749
- Harvey, P., Merín, B., Huard, T. L., et al. 2007, *ApJ*, 663, 1149
- Hatchell, J., Fuller, G. A., & Richer, J. S. 2007a, *A&A*, 472, 187, (Paper III)
- Hatchell, J., Fuller, G. A., Richer, J. S., Harries, T. J., & Ladd, E. F. 2007b, *A&A*, 468, 1009, (Paper II)
- Hatchell, J., Richer, J. S., Fuller, G. A., et al. 2005, *A&A*, 440, 151, (Paper I)
- Hirano, N., Kamazaki, T., Mikami, H., Ohashi, N., & Umemoto, T. 1999, in *Star Formation 1999, Proceedings of Star Formation 1999*, held in Nagoya, Japan, June 21 - 25, 1999, Editor: T. Nakamoto, Nobeyama Radio Observatory, p. 181–182, 181–182
- Johnstone, D., Di Francesco, J., & Kirk, H. 2004, *ApJ*, 611, L45
- Johnstone, D., Fich, M., Mitchell, G. F., & Moriarty-Schieven, G. 2001, *ApJ*, 559, 307
- Johnstone, D., Matthews, H., & Mitchell, G. F. 2006, *ApJ*, 639, 259
- Johnstone, D., Wilson, C. D., Moriarty-Schieven, G., et al. 2000, *ApJ*, 545, 327
- Jørgensen, J. K., Harvey, P. M., Evans, II, N. J., et al. 2006, *ApJ*, 645, 1246
- Jørgensen, J. K., Johnstone, D., Kirk, H., & Myers, P. C. 2007, *ApJ*, 656, 293
- Kirk, H., Johnstone, D., & Di Francesco, J. 2006, *ApJ*, 646, 1009
- Kirk, H., Johnstone, D., & Tafalla, M. 2007a, *ApJ*, 668, 1042
- Kirk, J. M., Ward-Thompson, D., & André, P. 2007b, *MNRAS*, 375, 843
- Kroupa, P. 2002, in *Astronomical Society of the Pacific Conference Series*, Vol. 285, *Modes of Star Formation and the Origin of Field Populations*, ed. E. K. Grebel & W. Brandner, 86
- Lada, C. J. & Lada, E. A. 2003, *ARA&A*, 41, 57
- Lai, S.-P., Evans, N. I., & coauthors. 2008, in prep.
- Larson, R. B. 1969, *MNRAS*, 145, 271
- Lay, O. P., Carlstrom, J. E., & Hills, R. E. 1995, *ApJ*, 452, L73
- Mac Low, M. & Klessen, R. S. 2004, *Reviews of Modern Physics*, 76, 125
- Morata, O., Girart, J. M., & Estalella, R. 2005, *A&A*, 435, 113
- Motte, F. & André, P. 2001, *A&A*, 365, 440
- Motte, F., André, P., & Neri, R. 1998, *A&A*, 336, 150
- Motte, F., André, P., Ward-Thompson, D., & Bontemps, S. 2001, *A&A*, 372, L41
- Motte, F., Bontemps, S., Schilke, P., et al. 2007, *A&A*, 476, 1243
- Myers, P. C. 1998, *ApJ*, 496, L109
- Nutter, D. & Ward-Thompson, D. 2007, *MNRAS*, 374, 1413
- O’Linger, J. C., Cole, D. M., Ressler, M. E., & Wolf-Chase, G. 2006, *AJ*, 131, 2601
- Padoan, P. & Nordlund, Å. 2002, *ApJ*, 576, 870
- Rebull, L. M., Stapelfeldt, K. R., Evans, II, N. J., et al. 2007, *ApJS*, 171, 447
- Reid, M. A. & Wilson, C. D. 2006, *ApJ*, 650, 970
- Rodríguez, L. F., Anglada, G., & Curiel, S. 1997, *ApJ*, 480, L125
- Rodríguez, L. F. & Reipurth, B. 1998, *Revista Mexicana de Astronomía y Astrofísica*, 34, 13
- Rosolowsky, E. W., Pineda, J. E., Foster, J. B., et al. 2007, *ArXiv e-prints*, 0711.0231
- Saraceno, P., André, P., Ceccarelli, C., Griffin, M., & Molinari, S. 1996, *A&A*, 309, 827
- Shirley, Y. L., Evans, II, N. J., & Rawlings, J. M. C. 2002, *ApJ*, 575, 337
- Siess, L., Forestini, M., & Bertout, C. 1997, *A&A*, 326, 1001
- Siess, L., Forestini, M., & Bertout, C. 1999, *A&A*, 342, 480
- Smith, M. D. 2000, *Irish Astronomical Journal*, 27, 25
- Swift, J. J. & Williams, J. P. 2008, *ArXiv e-prints*, 0802.2099
- Tassis, K. & Mouschovias, T. C. 2004, *ApJ*, 616, 283
- Testi, L. & Sargent, A. I. 1998, *ApJ*, 508, L91
- Vázquez-Semadeni, E., Kim, J., & Ballesteros-Paredes, J. 2005, *ApJ*, 630, L49
- Walsh, A. J., Myers, P. C., & Burton, M. G. 2004, *ApJ*, 614, 194
- Ward-Thompson, D., Di Francesco, J., Hatchell, J., et al. 2007, *PASP*, 119, 855
- Williams, J. P., de Geus, E. J., & Blitz, L. 1994, *ApJ*, 428, 693
- Wolf-Chase, G. A., Barsony, M., & O’Linger, J. 2000, *AJ*, 120, 1467
- Young, C. H., Shirley, Y. L., Evans, II, N. J., & Rawlings, J. M. C. 2003, *ApJS*, 145, 111